

See discussions, stats, and author profiles for this publication at: <https://www.researchgate.net/publication/260148428>

Facile Co-Assembly Process to Generate Core-Shell Nanoparticles with Functional Protein Corona

ARTICLE in BIOMACROMOLECULES · FEBRUARY 2014

Impact Factor: 5.75 · DOI: 10.1021/bm401819x · Source: PubMed

CITATIONS

13

READS

22

6 AUTHORS, INCLUDING:



Tao Li

Argonne National Laboratory

41 PUBLICATIONS 623 CITATIONS

[SEE PROFILE](#)



Qian Wang

University of South Carolina

106 PUBLICATIONS 4,406 CITATIONS

[SEE PROFILE](#)

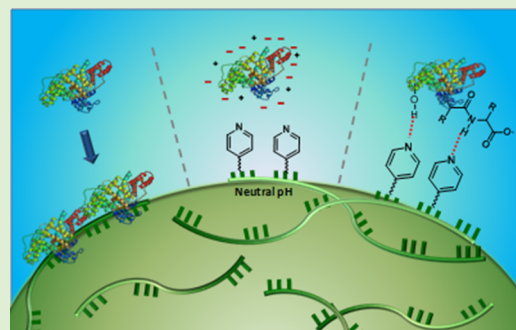
Facile Co-Assembly Process to Generate Core–Shell Nanoparticles with Functional Protein Corona

Nisaraporn Suthiwangcharoen,[†] Tao Li,[‡] Laying Wu,[§] Heidi B. Reno, Preston Thompson, and Qian Wang^{*}

Department of Chemistry and Biochemistry, University of South Carolina, Columbia, South Carolina 29208, United States

Supporting Information

ABSTRACT: A simple and robust protocol to maintain the structural feature of polymer–protein core–shell nanoparticles (PPCS-NPs) is developed based on the synergistic interactions between proteins and functional polymers. Using the self-assembly method, a broad range of proteins can be assembled to the selective water-insoluble polymers containing pyridine groups. The detailed analysis of the PPCS-NPs structure was conducted using FESEM and thin-sectioned TEM. The results illustrated that the protein molecules are located on the corona of the PPCS-NPs. While proteins are displacing between water and polymer to minimize the interfacial energy, the polymer offers a unique microenvironment to maintain protein structure and conformation. The proposed mechanism is based on a fine balance between hydrophobicity and hydrophilicity, as well as hydrogen bonding between proteins and polymer. The PPCS-NPs can serve as a scaffold to incorporate both glucose oxidase (GOX) and horseradish peroxidase (HRP) onto a single particle. Such a GOX-HRP bienzymatic system showed a ~20% increase in activity in comparison to the mixed free enzymes. Our method therefore provides a unique platform to preserve protein structure and conformation and can be extended to a number of biomolecules.



INTRODUCTION

The investigation of protein–polymer or protein–nanoparticle interaction is critical for the development of novel biomaterials and hierarchically assembled nanoarchitectures.^{1–7} Among them, the polymer–protein core–shell nanoparticles (PPCS-NPs) are the most common structures, which offer many advantages in the field of biomedical, sensing, and energy applications.² Current methods to synthesize such structures rely on the direct conjugation,^{7–13} direct self-assembly,^{14–16} physical adsorption of proteins on the surface of nanoparticles,^{17,18} electrostatic assembly,^{19–21} and affinity binding,^{22–24} as well as the assembly of peptide/protein–polymer conjugates.^{13,25–34} A covalent conjugation provides a strong protein attachment to polymers, yet the structure and bioactivity of proteins could be compromised during the reaction. On the other hand, the protein adsorption onto nanoparticles may lead to the “cryptic” peptide epitopes, resulting in a change in protein conformation and activity loss.^{17,18,35} Therefore, it still remains as a challenge to develop a robust one-step protocol which can control the structural feature of the PPCS-NPs while preserving protein activity and conformation, a critical feature for potential applications.^{2,3,36}

As the alternative noncovalent approach, we show that PPCS-NPs can be prepared by the self-assembly method based on synergistic interactions between proteins and selective polymers, such as poly(4-vinylpyridine) (P4VP) and pyridine grafted poly(hydroxyethyl methacrylate) (pHEMA). We have previously demonstrated that immiscible liquids or water–

polymer interfaces can be stabilized using protein cages^{37–41} where the protein cages were shown to be present on the corona.⁴² The assembly process is primarily entropically driven, with electrostatic interaction and hydrogen bonding as “patches” to stabilize the final structures. We hypothesize that a similar approach can be adapted to construct stable PPCS-NPs using functional proteins as corona, while the structure and functionality of proteins are preserved. This facile and versatile process can yield well-controlled core–shell structures with a broad range of functional proteins, in which the protein components stay at the corona. Our model proteins were shown to maintain as high as 90% of their original biological activities. We believe that the assembly between proteins and P4VP is driven by displacing proteins between the interface of water and polymers to minimize the interfacial energy, a similar process to the formation of Pickering emulsions.^{34,37,43–47} An optimal polymer structure is critical for a successful assembly since it provides a hydrophobic nature to promote the assembly as well as creates a benign microenvironment to assist the preservation of the conformation and activity of the proteins on the surface of the PPCS-NPs. The polymers containing pyridine units offer several advantages, including (i) the ability to hydrogen bond with proteins in a solution, which facilitates the self-assembly process, and (ii) the protonation ability,

Received: December 11, 2013

Revised: January 30, 2014

Published: February 3, 2014



which makes these polymers attractive candidates for drug delivery.⁴¹ Our method therefore offers a general route to prepare well-defined PPCS-NPs for potential biomedical and bioengineering applications.

EXPERIMENTAL SECTION

Materials. Poly(ethylene glycol) (PEG; M_w 10000), poly(vinyl alcohol) (PVA; M_w 30000–70000), poly(hydroxyethyl methacrylate) (pHEMA; M_w 20000), poly(acrylamide) (M_w 10000, 50 wt % in water), poly(acrylic acid) (M_w 100000, 35 wt % in water), P4VP (M_w 60000), P2VP (M_w 15600), *p*-nitrophenyl acetate, DMF, THF, poly- γ -benzyl-L-glutamate (PBLG; M_w 150000–300000), poly(lactic-co-glycolic acid) (PLGA; lactide/glycolide 50:50, M_w 30000–60000), poly(methyl methacrylate) (M_w 15000), and poly(*N*-isopropylacrylamide) (M_w 19000–30000) were purchased from Sigma-Aldrich company. Poly(vinylpyrrolidone) (PVP; M_w 1300000) were purchased from Alfa Aesar company. Polystyrene (PS; M_w 24600, PDI = 1.2) was obtained from Dr. Lavigne's lab at USC. P2VP₁₉₈-*b*-PCL₃₁₀ (the subscripts indicate the block lengths; PDI = 1.8) was purchased from Polymer Source Inc., Canada. O-Dianisidine was purchased from Alfa Aesar. Nicotinoyl chloride hydrochloride was purchased from TCI America. 4-Dimethylaminopyridine (DMAP) was purchased from Novabiochem. All the reagents were used as received. Water (18.2 MΩ) was obtained from Milli-Q system (Millipore).

Hemoglobin (Hem; from human), gelatin (Gel B; from bovine skin, Type B), concanavalin A (Con A; from *Canavalia ensiformis* (Jack bean), Type IV), α -chymotrypsin (ChT; from bovine pancreas Type II), avidin (Avi; from egg white), ovalbumin (Ova; albumin from chicken egg white, grade II), lipase (Lip; from *Candida rugosa*), papain (Pap; from papaya latex), ribonuclease A (Rib A; from bovine pancreas), trypsin (Try; from bovine pancreas, Type I), ferritin (Fer; from horse spleen, Type I), mucin (Psm; from porcine stomach, Type II), pepsin (Pep), and cytochrome c (Cyt) were purchased from Sigma-Aldrich company. Bovine serum albumin fraction V (BSA) and lysozyme (Lys; from hen egg white) were purchased from Rockland Company. Horseradish peroxidase (HRP) and streptavidin (Str) were purchased from Thermo Scientific. Albumin from human serum (HSA) was purchased from Fluka. Cowpea mosaic virus (CPMV), a 30 nm icosahedral particle, was isolated as previously reported.^{38,39} Glucose oxidase (GOX; from *Apergillus niger*, 100 u/mg) and horseradish peroxidase (HRP Type XII, 260 u/mg) were purchased from Sigma.

Analysis. Circular dichroism (CD) was performed on a Jasco 815 spectrophotometer, using a quartz cuvette with a 2 mm path length. Scans were taken from 180 to 250 nm at a rate of 100 nm·min⁻¹ with a 1 nm step resolution and a 1 s response. Four scans were conducted at a constant temperature of 25 °C, with a 10 min equilibration before the scans, and the average was reported. TEM analysis was performed by depositing 20 μ L aliquots of each sample with a concentration between 0.1 and 0.5 mg·mL⁻¹ onto 100-mesh carbon-coated copper grids for 2 min. The grids were then stained with 20 μ L of uranyl acetate (2% w/v) for 5 min and observed with a Hitachi H-8000 electron microscope. Cross-section TEM was performed using a modified protocol as reported previously.⁴² TEM thin sections were prepared by Sorvall MT2-B ultramicrotome. The images and elemental analysis of the cross sections were taken from mounted samples without staining. The specimen was treated with the protocol of glutaraldehyde fixation and acetone/resin infiltration prior to the analysis. Ultraplus FESEM equipped with in-lens detector, Hitachi H8000 TEM, JEOL JEM 2100F (200 kV) analytical TEM, and Libra 120 PLUS (120 kV) with in-column OMEGA energy filter. The zeta potential, hydrodynamic diameter and size distributions were measured with dynamic light scattering (DLS, Zetasizer Nano ZS, Malvern Instruments). The DLS was performed in triplicate with 15 runs recorded per measurement at 25 °C using a 4 mW He–Ne 633 nm laser module. The measurements were taken at 90° scattering angle. The particle size was measured without a further dilution or filtration. The deconvolution was accomplished using a non-negatively constrained least-squares fitting algorithm. All polydispersity index

(PDI) and zeta-potential values are averages of at least three measurements. UV-vis absorption studies were performed using an Agilent 8453 UV-vis spectrometer. The Eppendorf 5418 was used for centrifugation and particle purifications. All of the analyses were performed in at least triplicate, and the average was reported.

Typical Procedure to Synthesize P4VP-Protein Structures. A solution of P4VP (M_w 60000 Da) in dimethylformamide (DMF) or ethanol (2.0 mg·mL⁻¹, 0.2 mL) was slowly added into a solution of proteins in phosphate saline buffer (1× PBS; pH 7.4) with stirring. The final concentrations of P4VP and protein were 0.07 and 0.04 mg·mL⁻¹, respectively, and the volume percentage of DMF or ethanol was ~3%. To evaluate the effect of mass ratio of protein/polymer on the particle size and activity, the mass ratio of protein/P4VP = 0.57, 0.29, and 0.11 were prepared using the same procedure. The mixtures were placed at room temperature to allow ethanol to completely evaporate. If using DMF, the mixtures were dialyzed against PBS (2 × 1 L) with a 3500 molecular weight cutoff dialysis tubing (Pierce) for 48 h. To remove excess free proteins, the sample was subjected to centrifugation at 5–9 K rcf for 10 min depending upon the proteins.⁴⁸ The pellet was immediately resuspended in buffer solution. This step was repeated several times to ensure that most of the free proteins are removed. The percentage of proteins bound on the surface of the PPCS-NPs was calculated from the unbound proteins in the supernatant, by subtracting the amount of the unbound proteins from the initial amount of proteins used. In all of the systems described in the manuscript, the proteins bound on the surface of the PPCS-NPs was greater than 90% in comparison to the initial amount of the protein used. For the GOX/HRP bienzyme system, the particles were optimized to where the unbound enzymes were less than 5% (mass ratio of GOX/HRP/polymer = 0.2). Hence, the initial concentrations of GOX and HRP were used for assembly and the enzymatic assay without a further purification. The effect of the amount of the unbound enzyme is overcome by the presence of the particles. The final protein concentration was determined using a standard Lowry Assay. Various characterizations of samples were conducted thereafter. A similar procedure was performed with other polymers. Note that all polymers were dissolved in DMF, except PCL-*b*-P2VP, which was dissolved in THF.

CPMV- and ferritin-P4VP samples were prepared following the procedures reported previously.^{38,42} Briefly, a solution of P4VP in DMF (2 mg·mL⁻¹, 0.5 mL) was slowly added in to a solution containing CPMV or ferritin in PBS buffer while stirring. The samples were equilibrated at room temperature for at least 30 min then dialyzed against PBS (2 × 1 L) with a 3500 molecular weight cutoff dialysis tubing (Pierce) for 48 h. For the assembly at other conditions, sodium phosphate-citrate buffer (5 mM) was used for pH 2.2–8. Glycine-sodium hydroxide buffer (5 mM) was used for pH 8.6–10. Sodium bicarbonate–sodium hydroxide buffer (5 mM) was used for pH 12.

Activity Assay of Protein–Polymer Structures. For activity test of ChT and ChT-P4VP samples, all the experiments were performed in sodium phosphate buffer solutions (5.0 mM, pH 7.4), unless specified. The experiment was performed in a similar manner as previously reported.^{26,49} The functionality of ChT and the ChT-P4VP was determined by observing the absorbance associated with the hydrolysis product of *N*-succinyl-L-phenylalanine-*p*-nitroanilide (SPNA; purchased from Sigma Aldrich) in the presence of various sizes of the nanoparticles. At established time points, a SPNA stock solution in ethanol was added to the ChT-P4VP to reach the same final [ChT] and [SPNA] for both ChT-P4VP and native-free ChT. Activity assay was measured with the presence of ethanol by monitoring product formation for 30 min at 405 nm with a Molecular Device SPECTRAMax plus 384 with a microplate reader. The assays were performed multiple times, and the averages were reported. For activity assay of BSA and BSA-P4VP samples, all experiments were performed in potassium phosphate buffer (5.0 mM, pH 8.0), unless specified otherwise. The functionality of BSA and BSA-P4VP was examined by observing the absorbance of the hydrolysis of 4-nitrophenyl acetate in the presence of various sizes of the nanoparticles.⁵⁰ A 10 μ L solution of 10.0 mM 4-nitrophenyl acetate

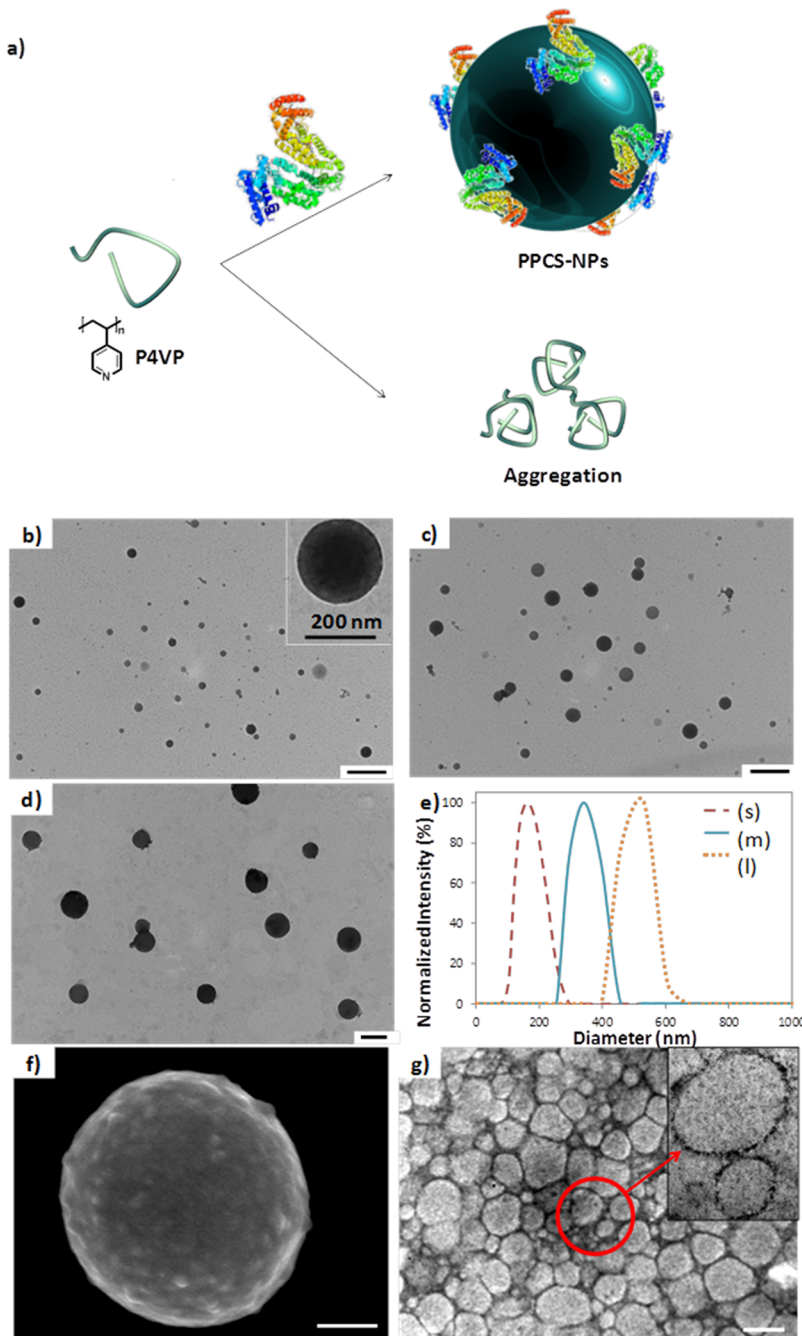


Figure 1. (a) Schematic representation of the formation of the PPCS-NPs in aqueous solution at pH 7.4. Without the presence of the proteins, the aggregation of P4VP was observed. (b–d) TEM images of BSA-P4VP (s), (m), and (l) with mass ratio of BSA/P4VP = 0.57, 0.29, and 0.11, respectively. (e) The average hydrodynamic size and the size distribution of BSA-P4VP (s), (m), and (l) from DLS measurement with the polydispersity index of 0.234, 0.285, and 0.400, respectively. (f, g) FESEM and thin-sectioned TEM image of ferritin-P4VP. Dark spots at the edge of the round samples belong to ferritin as indicated by red arrows. Scale bars = 500 nm for (b–d), 100 nm for (f), and 200 nm for (g).

in acetonitrile was dissolved in 0.94 mL buffer solution. Then, the mixture was gently mixed with a BSA or BSA-P4VP (50 μ L, [BSA] = 0.27 mM). The mixture was allowed to incubate in the dark at room temperature for 30 min, measured at the absorbance of 405 nm to evaluate the activity. The activity assays were performed in multiple trials, and the averages were reported. Similar methods were chosen for BSA-PCL-*b*-P2VP.

Enzymatic Activity Assay for GOX-P1. For the enzymatic studies, the particles were optimized to where the unbound enzymes were less than 3% (mass ratio of enzyme: polymer = 0.2). The initial concentrations of GOX and HRP were used for assembly and the enzymatic assay without a further purification. The enzymatic activity

was determined by UV-vis absorbance based on the oxidation of *o*-dianisidine which results in the change in the color of the solution. The procedure was adapted from previous literature.⁵¹ For each measurement, 2.5 mL of *o*-dianisidine (0.33 mM), 0.3 mL of glucose solution (5 mg·mL⁻¹), and 0.1 mL of 0.02% HRP solution were mixed in a quartz cell as a substrate. Then, 10 μ L of the same concentration of GOX-NP and free GOX was added to the solution mixture, and the absorption at 460 nm was recorded immediately for every 15 s interval for 2 min. Free GOX was used as a control. The GOX on the particles suspension and free GOX solution were adjusted at an approximately same concentration and volume to reduce systemic errors. For the bienzyme, the activity assay was measured in a similar manner but 110

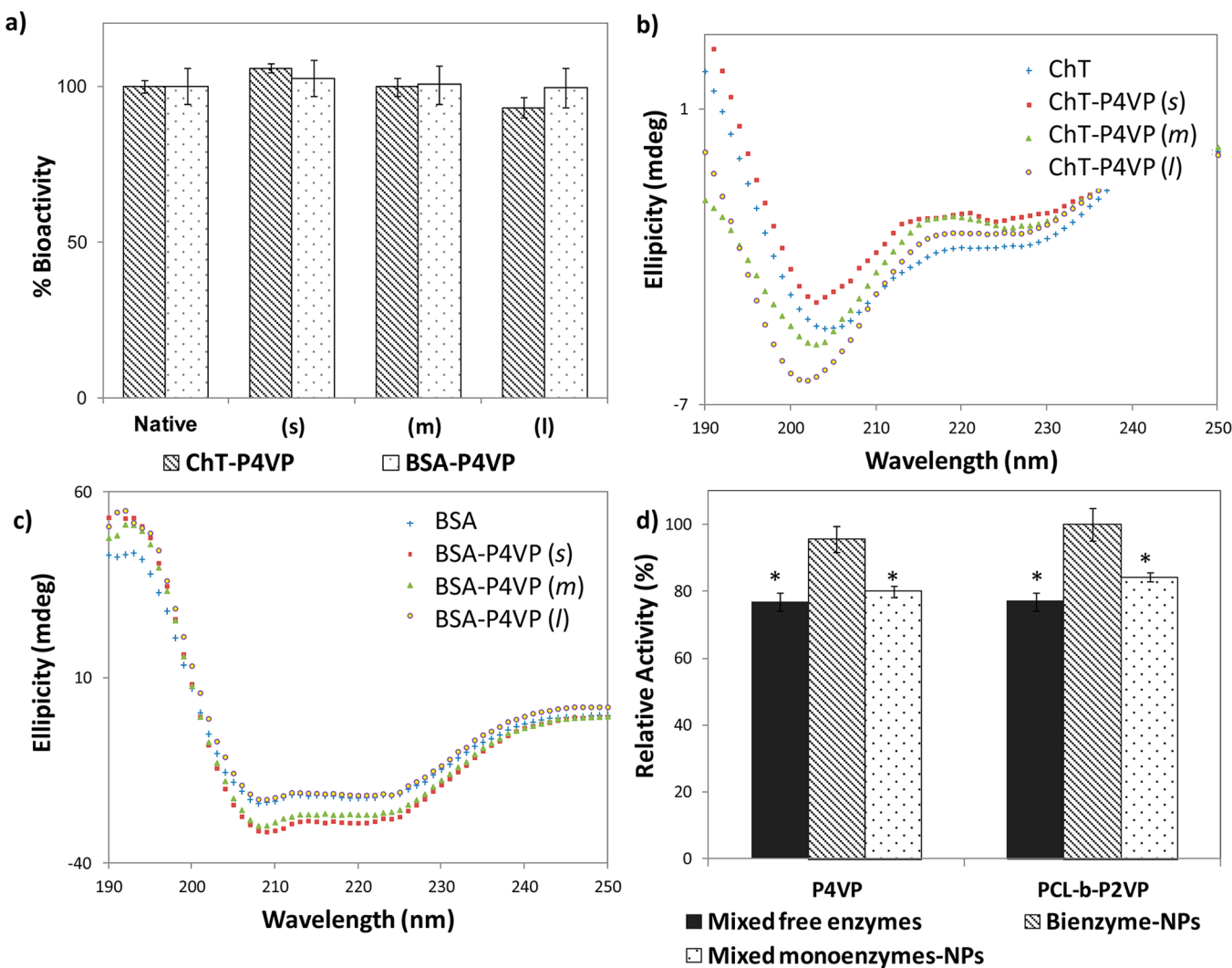


Figure 2. (a) Hydrolytic enzyme activity of ChT-P4VP and BSA-P4VP. The (s), (m), and (l) represent the particles from different sizes (small, medium, and large) and protein/polymer mass ratios. It shows that all proteins still maintain their functionalities after assembly. (b, c) CD spectra of different ChT-P4VP and BSA-P4VP, respectively. Native ChT shows two minima at 204 and 227 nm, while native BSA shows two minima at 208 and 223 nm. A slight blue shift was observed on ChT-P4VP, indicating the minor change of protein conformation. However, BSA-P4VP assembled PPCS-NPs still reveal two minima as shown in the native BSA, indicating that there is no significant conformational change of BSA after assembly. (d) Enzymatic activity assay of coassembly of bienzyme GOX/HRP with P4VP and PCL-*b*-P2VP, in comparison with mixture of free GOX and HRP and mixed monoenzyme-NPs at pH 7. The bienzyme-NPs exhibited the highest activity among others likely due to an increase in a spatial proximity of both enzymes. Error bars represent the standard error of the mean of triplicate samples (**p*-value < 0.05 vs bienzyme-NPs of each polymer).

μL of GOX-HRP-NP was added to the stock solution containing *o*-dianisidine and glucose prior to the measurement. The enzymatic activity of all samples was measured in a potassium phosphate buffer (0.1 M, pH 7).

RESULTS AND DISCUSSION

In a typical experiment, P4VP (60 K) was first employed to coassemble with a series of proteins that differ in isoelectric points (pI) and molecular weights (M_w ; Table S1; Figure 1a). The assembly was conducted by dropwise addition of P4VP in DMF or ethanol into the protein in buffer solution with stirring. Upon removing the organic solvent by dialysis or solvent evaporation, we observed that at neutral pH, low pI proteins, such as BSA, pepsin, or lipase, formed nicely dispersed particles with P4VP (Figure 1b–d, Figure S1), while high pI proteins, such as papain or lysozyme, resulted in aggregations (Figure S2). Although the presence of most proteins cannot be visualized with transmission electron microscope (TEM), the

absence of proteins showed only aggregations and precipitations of P4VP, which proved that proteins play a vital role in stabilizing the dispersion of P4VP in water. Since a control over the size of nanoparticles can be achieved by controlling the interfacial tension through the surface composition and concentration, the size of the particles and polydispersity index (PDI) values were shown to decrease as the mass ratio of BSA and P4VP ($M_{\text{BSA}}/M_{\text{P4VP}}$) increases, which is consistent with our previous report when viral particles were used in the assembly.⁴⁰ A higher mass ratio of the proteins to polymer leads to a lower interfacial tension and therefore smaller particles can be generated compared to a lower protein/polymer ratio. The particles are typically stable in solution for about 1–2 weeks at room temperature and 4 weeks at 4 °C.

Since it is quite difficult to visualize proteins under microscope, we assembled P4VP with cowpea mosaic virus (CPMV, a 30 nm icosahedral viral particle) or horse-spleen ferritin (a 12 nm protein particle with an iron oxide core that

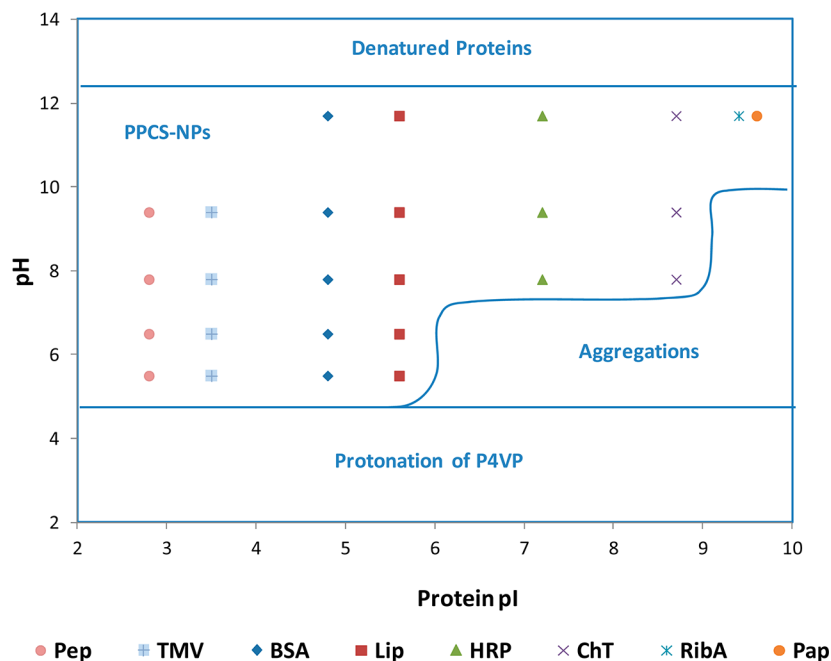


Figure 3. Pseudophase diagram representing the transitions in the proteins-P4VP structures: aggregations of proteins-P4VP; protonation of P4VP leading a homogeneous solution; colloids of proteins-P4VP; and denatured proteins. The data points indicated successful assembly between proteins and P4VP at a particular pH.

can induce the electron density upon the microscope visualization). With CPMV, the PPCS-NPs exhibit spherical morphology with a rough surface, indicating the presence of CPMV on the corona (Figure S3a,b). Further analyses were also conducted using thin-sectioned TEM and energy-dispersive X-ray spectroscopy (EDS) to analyze the in-depth structure of CPMV-P4VP (Figure S3c–f). Without staining, CPMV exhibits a low contrast under TEM. By using EDS, the S and P peaks, which belong to RNA and proteins of CPMV, were only found at the outmost shell of the CPMV-P4VP, while no S and P were detected in the center of the thin-sectioned structure. To confirm that proteins are also present on the corona, ferritin was selected as a probe. Figure 1f shows a representative FESEM image of ferritin-P4VP. Detailed structural analysis was conducted using the thin-sectioned TEM, displaying a round-shaped thin-sectioned structure surrounded by small dark particles (Figure 1g). This clear boundary at the interface resulted from a high contrast of ferritin under TEM. By using energy-filtered TEM imaging and iron element mapping, we previously reported that the dark spot was composed of ferritin, whereas the white area in the center was mainly P4VP.⁴²

Having established that proteins are located on the corona of the PPCS-NPs, the structure and functionality of the proteins after assembly were analyzed using Chymotrypsin (ChT) and BSA as model proteins. The samples were prepared in three different sizes, (*s*, *m*, and *l*) for small, medium, and large, by adjusting the protein/P4VP ratio to investigate the effect of particle size on the activity. The activity assays are based on the increase in fluorescent emission or absorbance of products accompanying the ChT- and BSA-catalyzed hydrolysis of their substrate, respectively (Scheme S1). ChT activities in ChT-P4VP (*s*, *m*, and *l*) were similar to that of the native free ChT at the same concentration (Figure 2a). The size changes in ChT-P4VP samples did not significantly affect the bioactivity of ChT. Despite the fact that free ChT is denatured upon a rapid

stirring,⁵² our PPCS-NPs are shown to protect the ChT from being denatured under such circumstance. Similar results were observed when using BSA. In addition, circular dichroism (CD) spectra revealed that BSA and ChT still maintain their original folded conformations to a great extent after assembly (Figure 2b,c).^{26,52} These results demonstrate that various proteins can assemble with P4VP to form PPCS-NPs while preserving structural and functional features of the proteins.

Encouraged by the preserved catalytic activity and stability of BSA and ChT after assembling to the NPs, we next investigated whether a similar procedure can be applied to construct a multienzyme-NP system and whether all enzymes still maintain their functionality as they are on the same particles, thus forming a multifunctional “enzymosome.” As a proof of concept, glucose oxidase (GOX) and horseradish peroxidase (HRP) were chosen as a model bienzymatic system to assemble with P4VP or poly(caprolactone)-block-poly(2-vinylpyridine) (PCL-*b*-P2VP). Under a neutral condition with the mass ratio of enzyme/polymer = 0.2, well-dispersed spherical particles were obtained with a hydrodynamic diameter of about 150–250 nm using either GOX or HRP individually or a mixture of both enzymes under different mixing ratios (Figure S4). The activity assays were performed by adding bienzyme-NPs to the stock solution containing *o*-dianisidine and glucose at room temperature (for the mechanism of the assay, see Scheme S2). The absorbance of the oxidized *o*-dianisidine was monitored at 460 nm while a mixed monoenzyme-NPs (a mixture of GOX-NPs and HRP-NPs) and a mixture of free GOX and HRP were used as control studies with the same concentration and ratios of GOX/HRP. Figure 2d illustrates the relative activities of mixed free enzymes, mixed monoenzyme-NPs, and bienzyme-NPs at GOX/HRP = 4:1. The activity of the enzymes on the NPs was shown to be higher than that of the free enzymes, while the bienzyme-NPs exhibited the highest activity among all. Due to an increase in proximity of both GOX and HRP on the bienzyme-NP system, we rationalized that the H₂O₂

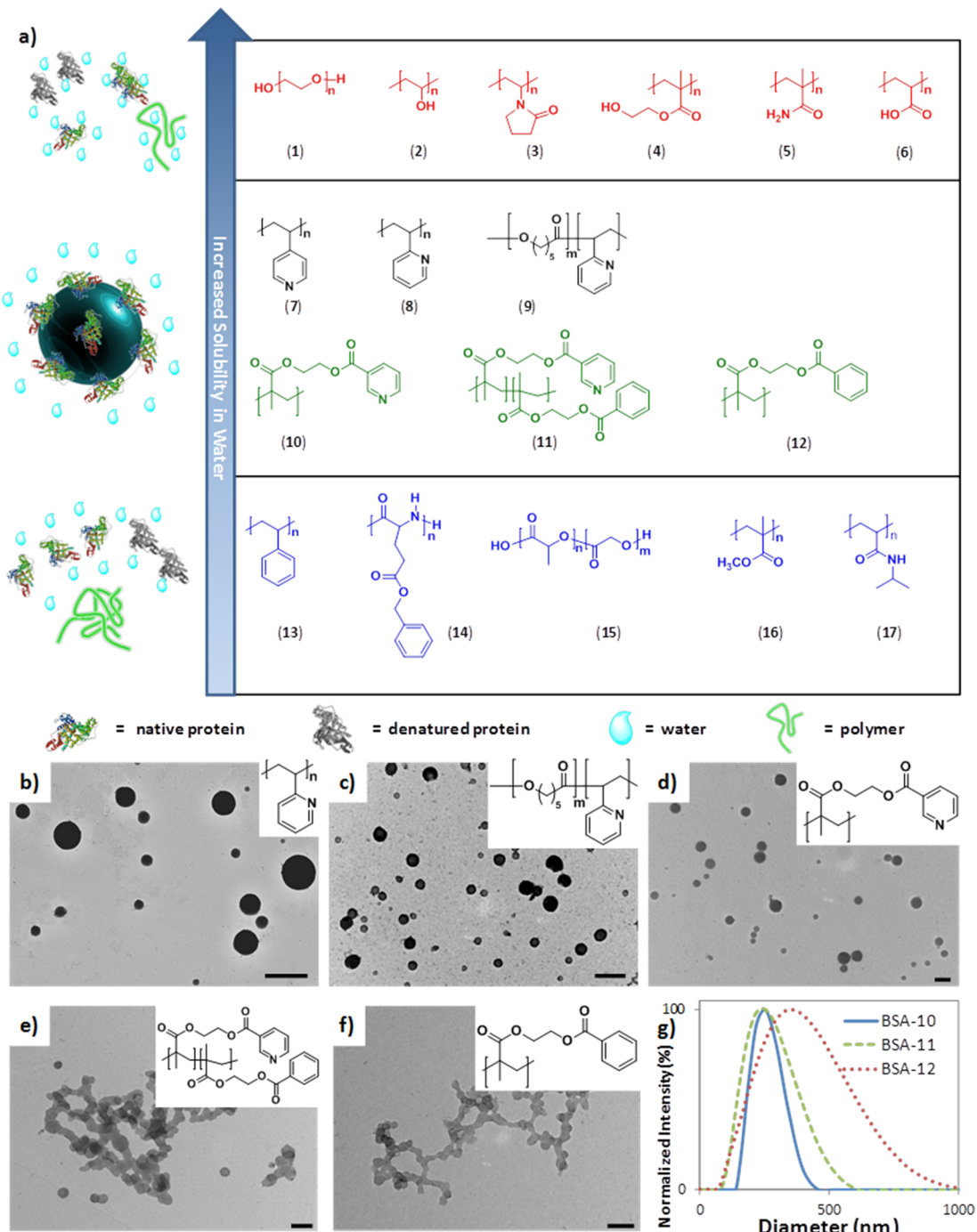


Figure 4. (a) Chemical structures of polymers used in the assembly of PPCS-NPs. No assembly was observed when hydrophilic neutral polymers (1–6) were employed while highly hydrophobic polymers (12–17) led to aggregations due to a lack of interaction between proteins and polymers. The assembly occurs when water-insoluble polymer containing pyridine units are used (7–11). (b–f) TEM images of BSA with polymers at a neutral pH. More aggregation was observed as the ratio of pyridine groups decreased. The scale bars = 250 nm. (g) DLS analysis revealed the hydrodynamic sizes of BSA assembled with polymers 10–12, that is, BSA-10, BSA-11, and BSA-12, with the PDI = 0.267, 0.312, and 0.773, respectively.

molecules producing from the oxidation of glucose were enriched around the surface of the NPs, thus, having more accessibility to the HRP, resulting in an increase in the enzymatic activity in comparison to the mixture of mono-enzyme-NPs or the mixture of the free enzymes.^{53,54} This finding suggests that the PPCS-NPs can preserve but also enhance the activity of the enzymes due to an increase in spatial proximity and enzyme localization on the particles.⁵⁴

To better understand the assembly process, we altered the pH of the solution to control surface charges of proteins and see how it could impact the assembly of proteins with different pIs with P4VP. As summarized in Figure 3, in all situations, colloids were evident only at pH > pI, where proteins carry a net negative charge; while aggregations were observed at pH < pI. On the other hand, neither colloidal particle was observed at pH < 3 due to an increase in solubility of P4VP resulting from

the protonation of the pyridine units,⁴¹ while the denaturation of proteins was observed at pH > 10 (see Figure S5). These observations suggest that the assembly process is pH-dependent, and negatively charged proteins are required for a successful assembly with P4VP. To further investigate whether the electrostatic interaction plays a role in protein–polymer assembly, we adjusted the ionic strength of the assembly solution by the addition of NaCl (0–1.0 M) prior to the assembly. Although an increase in size was observed in the presence of NaCl (Figure S6), colloidal particles were still obtained, indicating that electrostatic interactions are not sufficient to account for the formation of PPCS-NPs. A controlled study was performed by adding NaCl after the PPCS-NPs were formed, and similar results were obtained (data not shown). The size increases as the ionic strength increases suggested that the PPCS-NPs were stabilized by the electrostatic effect from the negatively charged proteins, which create a repulsive interaction between particles. Upon the addition of NaCl, the surface charge of the proteins was screened, thereby minimizing a repulsive interaction between particles. As a result, an increase in size was observed.

At a typical assembly condition, although proteins are negatively charged, the P4VP is near neutral; therefore, the formation of PPCS-NPs is unlikely due to the electrostatic interaction between proteins and P4VP molecules. We hypothesize that the assembly between protein and P4VP is driven by displacing proteins (serving as amphiphiles) between the interface of water and P4VP, which is mostly deprotonated at a pH > 5, to minimize the interfacial energy, a similar process to the formation of Pickering emulsions.^{37,38,44} On the other hand, an optimal polymer structure is critical for a successful assembly since it provides a hydrophobic nature to drive the assembly while creating a benign microenvironment to assist the conformational preservation of proteins. To further investigate the interaction between protein and polymer, various types of polymers were tested as shown in Figure 3a. No assembly was observed when hydrophilic polymers (**1–6**) were employed, while highly hydrophobic polymers (**13–17**) led to aggregations likely due to a lack of interaction between proteins and polymers. Upon analyzing the composition of the aggregations by ninhydrin assay, no protein was found.

A closer look at the polymer structures allowed us to demonstrate that the polymers containing a pyridine unit, such as P4VP (**7**), poly(2-vinylpyridine) (P2VP; **8**), or PCL-*b*-P2VP (**9**), are able to spontaneously self-assemble with proteins to form spherical colloidal particles (Figure 4b,c, Table S2). We hypothesize that such interaction is governed by H-bonding as the pyridine units of P4VP can readily serve as a hydrogen bond donor or acceptor.^{55,56} To confirm our hypothesis, a newly synthesized pyridine-grafted poly(2-hydroxyethyl methacrylate) (pHEMA; **10**) and its structural analogues (**11** and **12**) were used to assemble with BSA (see Supporting Information and Figure S7 for detailed synthesis). Similar to that of P4VP, the assembly of (**10**) and BSA resulted in spherical particles (Figure 4d). More aggregation and larger size distributions were observed under TEM and DLS as the number of the benzene units increased (Figure 4e–g). The aggregation of benzene-derivatized pHEMA (**12**) was evident within the first couple hours after mixing with proteins (Figure 4f).

Due to the fact that urea has the ability to disrupt the H-bonding on proteins,^{57,58} further studies were carried out with the incorporation of urea during assembly to investigate the

role of H-bonding in the process. The experiment was conducted in two different routes: (i) BSA was premixed with urea prior to assembly with P4VP and (ii) the BSA-P4VP particles were preformed followed by the addition of urea (0.1–10 M). In both conditions, urea caused the aggregation and precipitation of the protein/polymer mixtures (Figure S8). The secondary structures of BSA and BSA-P4VP after a urea treatment were analyzed using a CD spectroscopy, and the results showed a decrease of the 222 minimum, indicating a protein unfolding upon the presence of urea (Figure S8a,b). Since the disassembly could also be resulted from the denaturation of the proteins, the BSA was heated at 95 °C for 10 min to allow the BSA to be fully denatured prior to the assembly while still maintain its ability to hydrogen bond with other substances. The results showed that the colloidal particles can still be formed (Figure S8e). We rationalized that although the heating causes the denaturation of BSA, unlike urea, it did not prevent the interaction of BSA with P4VP through H-bonding.

CONCLUSION

In summary, we have developed a facile one-step self-assembly method to create PPCS-NPs with a well-defined structure and a controllable size while proteins preserve their biological structures and functionality. The assembly is governed by H-bonding and a fine balance between hydrophobicity and hydrophilicity of the polymers. While the protein component displaces between water and the polymer component to minimize the interfacial energy, the polymer component offers a unique microenvironment for the retaining of the protein conformation and functionality. Furthermore, using GOX and HRP as a model bienzymatic system, we have demonstrated that our PPCS-NPs can serve as a readily achievable scaffold to incorporate both enzymes onto a single NP with about a 20% increase in activity in comparison to the mixed free enzymes. Considering the significance of protein and enzyme compartmentation,^{59,60} our method will open up new avenues in the preparation of protein-based nanostructures for delivery, imaging, sensing, catalysis, and other biomedical/biotechnical applications.

ASSOCIATED CONTENT

Supporting Information

Lists of proteins used in the construction of PPCS-NPs and further assembly results; detailed analysis of the PPCS-NPs; synthesis of the bienzyme nanoparticles; representative TEM images, activity assay, and CD analysis of PPCS-NPs under different conditions; mechanism investigation of the formation of PPCS-NPs; CD spectra and relative activity of BSA exposed to different urea concentration; synthesis of pyridine-derivatized pHEMA and its structural analogue. This material is available free of charge via the Internet at <http://pubs.acs.org>.

AUTHOR INFORMATION

Corresponding Author

*E-mail: wang263@mailbox.sc.edu.

Present Addresses

[†]Molecular Sciences and Engineering Team, U.S. Army, Natick Soldier Research, Development and Engineering Center, Natick, MA 01760, United States (N.S.).

[‡]X-ray Science Division, Argonne National Laboratory, 9700 Cass Ave., Lemont, IL 60439, United States (T.L.).

[§]Montclair State University, 1 Normal Ave, Montclair, NJ 07043, United States (L.W.).

Notes

The authors declare no competing financial interest.

The manuscript was written through contributions of all authors. Nisaraporn Suthiwangcharoen and Tao Li contributed equally to the work.

ACKNOWLEDGMENTS

We thank Drs. Ken Shimizu and Yao Lin for helpful discussions. This work was supported by the US NSF CHE-0748690 and CHE-1307319.

REFERENCES

- (1) Ge, J.; Lei, J.; Zare, R. N. *Nat. Nanotechnol.* **2012**, *7*, 428–432.
- (2) Mahmoudi, M.; Lynch, I.; Ejtehadi, M. R.; Monopoli, M. P.; Bombelli, F. B.; Laurent, S. *Chem. Rev.* **2011**, *111*, 5610–5637.
- (3) Lynch, I.; Dawson, K. A. *Nano Today* **2008**, *3*, 40–47.
- (4) Zhang, K.; Zheng, D.; Hao, L.; Cutler, J. I.; Auyeung, E.; Mirkin, C. A. *Angew. Chem., Int. Ed.* **2012**, *51*, 1169–1172.
- (5) Yan, M.; Du, J.; Gu, Z.; Liang, M.; Hu, Y.; Zhang, W.; Priceman, S.; Wu, L.; Zhou, Z. H.; Liu, Z.; Segura, T.; Tang, Y.; Lu, Y. *Nat. Nanotechnol.* **2010**, *5*, 48–53.
- (6) Monopoli, M. P.; Aberg, C.; Salvati, A.; Dawson, K. A. *Nat. Nanotechnol.* **2012**, *7*, 779–786.
- (7) De, M.; Rana, S.; Akpinar, H.; Miranda, O. R.; Arvizo, R. R.; Bunz, U. H. F.; Rotello, V. M. *Nat. Chem.* **2009**, *1*, 461–465.
- (8) Tao, L.; Mantovani, G.; Lecolley, F.; Haddleton, D. M. *J. Am. Chem. Soc.* **2004**, *126*, 13220–13221.
- (9) Heredia, K. L.; Bontempo, D.; Ly, T.; Byers, J. T.; Halstenberg, S.; Maynard, H. D. *J. Am. Chem. Soc.* **2005**, *127*, 16955–16960.
- (10) Heredia, K. L.; Maynard, H. D. *Org. Biomol. Chem.* **2007**, *5*, 45–53.
- (11) Rana, S.; Yeh, Y.-C.; Rotello, V. M. *Curr. Opin. Chem. Biol.* **2010**, *14*, 828–834.
- (12) Mougin, N. C.; van Rijn, P.; Park, H.; Muller, A. H. E.; Boker, A. *Adv. Funct. Mater.* **2011**, *21*, 2470–2476.
- (13) van Rijn, P.; Park, H.; Nazli, K. O.; Mougin, N. C.; Boker, A. *Langmuir* **2013**, *29*, 276–284.
- (14) Payne, G. F.; Kim, E.; Cheng, Y.; Wu, H. C.; Ghodssi, R.; Rubloff, G. W.; Raghavan, S. R.; Culver, J. N.; Bentley, W. E. *Soft Matter* **2013**, *9*, 6019–6032.
- (15) Ghosh, A.; Guo, J. C.; Brown, A. D.; Royston, E.; Wang, C. S.; Kofinas, P.; Culver, J. N. *J. Nanomater.* **2012**, *2012*, 1–6.
- (16) Gerasopoulos, K.; Pomerantseva, E.; McCarthy, M.; Brown, A.; Wang, C.; Culver, J. N.; Ghodssi, R. *ACS Nano* **2012**, *6*, 6422–6432.
- (17) Gebauer, J. S.; Malissek, M.; Simon, S.; Knauer, S. K.; Maskos, M.; Stauber, R. H.; Peukert, W.; Treuel, L. *Langmuir* **2012**, *28*, 9673–9679.
- (18) Klein, J. *Proc. Natl. Acad. Sci. U.S.A.* **2007**, *104*, 2029–2030.
- (19) Kostainen, M. A.; Hiekkataipale, P.; Laiho, A.; Lemieux, V.; Seitsonen, J.; Ruokolainen, J.; Ceci, P. *Nat. Nanotechnol.* **2013**, *8*, 52–56.
- (20) Sharma, K. P.; Collins, A. M.; Perriman, A. W.; Mann, S. *Adv. Mater.* **2013**, *25*, 2005–2010.
- (21) Gallat, F. X.; Brogan, A. P. S.; Fichou, Y.; McGrath, N.; Moulin, M.; Hartlein, M.; Combet, J.; Wuttke, J.; Mann, S.; Zaccai, G.; Jackson, C. J.; Perriman, A. W.; Weik, M. *J. Am. Chem. Soc.* **2012**, *134*, 13168–13171.
- (22) Dirks, A. J.; Nolte, R. J. M.; Cornelissen, J. *Adv. Mater.* **2008**, *20*, 3953–3957.
- (23) Hannink, J. M.; Cornelissen, J.; Farrera, J. A.; Fouquet, P.; De Schryver, F. C.; Sommerdijk, N.; Nolte, R. J. M. *Angew. Chem., Int. Ed.* **2001**, *113*, 4868–4870.
- (24) Boerakker, M. J.; Botterhuis, N. E.; Bomans, P. H. H.; Frederik, P. M.; Meijer, E. M.; Nolte, R. J. M.; Sommerdijk, N. *Chem.—Eur. J.* **2006**, *12*, 6071–6080.
- (25) De, M.; Miranda, O. R.; Rana, S.; Rotello, V. M. *Chem. Commun.* **2009**, *2157*–2159.
- (26) De, M.; Rotello, V. M. *Chem. Commun.* **2008**, *3504*–3506.
- (27) De, M.; Rana, S.; Rotello, V. M. *Macromol. Biosci.* **2009**, *9*, 174–178.
- (28) van Eldijk, M. B.; Wang, J. C. Y.; Minten, I. J.; Li, C.; Zlotnick, A.; Nolte, R. J. M.; Cornelissen, J. J. L. M.; van Hest, J. C. M. *J. Am. Chem. Soc.* **2012**, *134*, 18506–18509.
- (29) Kim, K. T.; Meeuwissen, S. A.; Nolte, R. J. M.; van Hest, J. C. M. *Nanoscale* **2010**, *2*, 844–858.
- (30) Ryadnov, M. G. *Angew. Chem., Int. Ed.* **2007**, *46* (6), 969–972.
- (31) Klem, M. T.; Mosolf, J.; Young, M.; Douglas, T. *Inorg. Chem.* **2008**, *47*, 2237–2239.
- (32) Huang, X.; Li, M.; Green, D. C.; Williams, D. S.; Patil, A. J.; Mann, S. *Nat. Commun.* **2013**, *4*, DOI: 10.1038/ncomms3239.
- (33) Velonia, K.; Rowan, A. E.; Nolte, R. J. M. *J. Am. Chem. Soc.* **2002**, *124*, 4224–4225.
- (34) van Rijn, P.; Mougin, N. C.; Franke, D.; Park, H.; Boker, A. *Chem. Commun.* **2011**, *47*, 8376–8378.
- (35) Lynch, I.; Dawson, K. A.; Linse, S. *Sci. STKE* **2006**, *327*, 14.
- (36) Lynch, I.; Cedervall, T.; Lundqvist, M.; Cabaleiro-Lago, C.; Linse, S.; Dawson, K. A. *Adv. Colloid Interface Sci.* **2007**, *134*–135, 167–174.
- (37) Russell, J. T.; Lin, Y.; Böker, A.; Su, L.; Carl, P.; Zettl, H.; He, J.; Sill, K.; Tangirala, R.; Emrick, T.; Littrell, K.; Thiagarajan, P.; Cookson, D.; Fery, A.; Wang, Q.; Russell, T. P. *Angew. Chem., Int. Ed.* **2005**, *44*, 2420–2426.
- (38) Li, T.; Niu, Z.; Emrick, T.; Russell, T. R.; Wang, Q. *Small* **2008**, *4*, 1624–1629.
- (39) Li, T.; Wu, L.; Suthiwangcharoen, N.; Bruckman, M. A.; Cash, D.; Hudson, J. S.; Ghoshroy, S.; Wang, Q. *Chem. Commun.* **2009**, *2869*–2871.
- (40) Li, T.; Ye, B.; Niu, Z.; Thompson, P.; Seifert, S.; Lee, B.; Wang, Q. *Chem. Mater.* **2009**, *21*, 1046–1050.
- (41) Suthiwangcharoen, N.; Li, T.; Li, K.; Thompson, P.; You, S. J.; Wang, Q. *Nano Res.* **2011**, *4*, 483–493.
- (42) Wu, L.; Li, T.; Blom, D.; Zhao, J.; Ghoshroy, S.; Wang, Q. *Microsc. Res. Tech.* **2011**, *74*, 636–641.
- (43) Tangirala, R.; Hu, Y.; Joralemon, M.; Zhang, Q.; He, J.; Russell, T. P.; Emrick, T. *Soft Matter* **2009**, *5*, 1048–1054.
- (44) Niu, Z.; He, J.; Russell, T. P.; Wang, Q. *Angew. Chem., Int. Ed.* **2010**, *49*, 10052–10066.
- (45) Binks, B. P.; Lumsdon, S. O. *Langmuir* **2000**, *16*, 8622–8631.
- (46) Pieranski, P. *Phys. Rev. Lett.* **1980**, *45*, 569–572.
- (47) Lin, Y.; Skaff, H.; Emrick, T.; Dinsmore, A. D.; Russell, T. P. *Science* **2003**, *299*, 226–229.
- (48) Das, R. K.; Kasoju, N.; Bora, U. *Nanomedicine* **2010**, *6*, 153–160.
- (49) You, C.; De, M.; Han, G.; Rotello, V. M. *J. Am. Chem. Soc.* **2005**, *127*, 12873–12881.
- (50) De, P.; Li, M.; Gondi, S. R.; Sumerlin, B. S. *J. Am. Chem. Soc.* **2008**, *130*, 11288–11289.
- (51) Li, D.; He, Q.; Cui, Y.; Duan, L.; Li, J. *Biochem. Biophys. Res. Commun.* **2007**, *355*, 488–493.
- (52) Jordan, B. J.; Hong, R.; Gider, B.; Hill, J.; Emrick, T.; Rotello, V. M. *Soft Matter* **2006**, *2*, 558–560.
- (53) Jia, F.; Zhang, Y. J.; Narasimhan, B.; Mallapragada, S. K. *Langmuir* **2012**, *28*, 17389–17395.
- (54) Jia, F.; Narasimhan, B.; Mallapragada, S. K. *Angew. Chem., Int. Ed.* **2013**, *59*, 355–360.
- (55) Nie, L.; Liu, S.; Shen, W.; Chen, D.; Jiang, M. *Angew. Chem., Int. Ed.* **2007**, *119*, 6437–6440.
- (56) Chen, D.; Jiang, M. *Acc. Chem. Res.* **2005**, *38*, 494–502.
- (57) Hua, L.; Zhou, R.; Thirumalai, D.; Berne, B. J. *Proc. Natl. Acad. Sci. U.S.A.* **2008**, *105*, 16928–16933.
- (58) Rezus, Y. L. A.; Bakker, H. J. *Proc. Natl. Acad. Sci. U.S.A.* **2006**, *103*, 18417–18420.
- (59) O’Neil, A.; Reichhardt, C.; Johnson, B.; Prevelige, P. E.; Douglas, T. *Angew. Chem., Int. Ed.* **2011**, *50*, 7425–7428.

(60) de la Escosura, A.; Nolte, R. J. M.; Cornelissen, J. J. L. M. *J. Mater. Chem.* **2009**, *19*, 2274–2278.